

# EFFECT OF COMPOSITION ON THE RECRYSTALLIZATION BEHAVIOR OF IF STEELS DURING SIMULATED HOT STRIP ROLLING

A. Najafi-Zadeh

Department of Materials Engineering  
Isfahan University of Technology  
Isfahan, Iran

J.J. Jonas

Department of Metallurgical Engineering  
McGill University, Montreal  
Canada

**Abstract** Flow curves are generated in multi-pass torsion tests for a titanium stabilized and a niobium stabilized IF steel. Two types of test schedule are used, one based on plate rolling and the other approximating strip rolling. The purpose of the former is to define the three critical temperatures of steel rolling. The strip schedules are varied in order to investigate the influence of increasing the total finishing strain (from 2.1 to 3.2) and lowering the first finishing pass temperature (from 990 to 930°C) on microstructural evolution in these steels. All the tests are carried out at a strain rate of 2s<sup>-1</sup>. Under hot strip rolling conditions, static recrystallization is responsible for the high degree of interpass softening. During the final passes, dynamic recrystallization occurs to a degree that depends on the composition of the steel, the total finishing strain and the temperature. Subjected to the same strip rolling schedule, the niobium stabilized steel has a finer ferrite grain size than the IF steel stabilized with titanium.

**چکیده** به کمک آزمایش پیچش فرآیند نورد گرم، ورق و تسمه بر روی فولادهایی بدون عناصر بین نشینی که حاوی تیتانیوم و یا نایابیوم میباشند شبیه سازی گردید. هدف از شبیه سازی نورد ورق تعیین دماهای بحرانی این فولادها و منظور از شبیه سازی نورد تسمه تعیین اثرات افزایش مجموع کرنش های نهایی (از ۲/۱ تا ۳/۲) و درجه حرارت اولین عبور قفسه نهایی از ۹۳۰°C تا ۹۹۰°C روی تغییرات ریزساختاری محصول بوده است. کلیه آزمایشات به سرعت کرنش ۲/S انجام گرفته است. نتایج آزمایشات روی نورد تسمه نشان داد که مکانیزم اصلی نرم شدن این فولادها در زمان بین عبورهای اولیه عمدتاً تبلور مجدد استاتیکی است در صورتیکه در عبورهای نهایی تبلور مجدد دینامیکی رخ میدهد که میزان آن وابسته به ترکیب شیمیایی، دمای عبور نهایی و مقدار کل کرنش در این عبورها است. نتیجه این تحقیق همچنین نشان داد که در شرایط یکسان نورد تسمه فولاد تیتانیوم دار دارای دانه های فریت ریزتری نسبت به فولاد نایابیوم دار خواهد بود.

## INTRODUCTION

The chemical composition, slab reheating temperature for hot rolling, as well as the rolling speed, total finishing reduction, and finishing and coiling temperatures all influence the final properties of IF steels. The composition determines the kind of precipitate that forms and the rolling parameters affect its size distribution. For example, Gupta et al. [1] have shown that at low slab reheating temperatures, the coarse precipitates formed in Ti-IF steels after casting are not dissolved, while high slab reheating temperatures lead to subsequent reprecipitation which is relatively fine and dense.

The effect of chemical composition has been investigated by numerous authors [2,5] but that of the total

finishing strain and of the finishing temperatures in hot strip rolling has rarely been studied. Hashimoto et al. [6] have shown that higher reductions and more passes during finish rolling improve the ductility and formability of Nb-IF steels. The beneficial effects of higher reductions and increased rolling speeds are believed to be related to promotion of the strain induced precipitation of NbCN during rolling; these authors have shown that a combination of high reductions during finish rolling and early run-out table cooling are essential to achieving high ductilities in Nb-IF steels by promoting fine and uniform grain sizes.

Bleck et al. [7] have also shown that decreasing the finishing temperature in the austenite region results in a finer ferrite grain size. As IF steels have high A<sub>F3</sub> temperatures (~880 to 900°C), of the finishing temperature is too

low, on the other hand, the transformation of austenite to ferrite takes place during rolling, leading to a sudden drop in flow stress [2,8] which makes hot-band gauge control difficult.

This paper discusses the effects of hot rolling parameters on the behavior of Ti and Nb based IF steels. In this context, we also examine the differences between the strip and plate rolling behaviors of these steels. Other aspects of the study concern:

- (1) determination of the three critical temperatures of hot-rolling, i.e. the no-recrystallization temperature, and the temperatures associated with the start and end of the austenite-to-ferrite transformation ( $T_{nr}$ ,  $A_{r3}$  and  $A_{r1}$ , respectively);
- (2) investigation of the possible occurrence of dynamic recrystallization during the simulated strip rolling of IF steels; and
- (3) clarification of the effect of temperature and total finishing pass strain on the ferrite grain size of these steels under strip rolling conditions.

## MATERIALS AND EXPERIMENTAL PROCEDURE

The chemical compositions of the two IF steels studied are given in Table 1. These have the same base composition of approximately 0.004 wt% carbon, 0.03 wt% silicon, 0.15 wt% manganese, and 0.003 wt% nitrogen. The major difference in composition involved the type of carbon stabilizing element employed, i.e. titanium or niobium; approximately 0.06 wt% being used in both cases.

The present materials were taken from as-cast slabs supplied by Stelco Steel, in Hamilton, Ontario. Torsion test specimens, with a gauge length of 23 mm and 6.2 mm in diameter were machined from the slabs. The torsion experiments were performed on a servo-hydraulic, com-

**TABLE 1. Chemical Compositions of the Two IF Steels (wt %).**

Steel Code	C	Si	Mn	S	N	Ti	Nb
A	.0035	.022	.15	.012	.003	.065	—
B	.0036	.024	.16	.013	.003	—	.056

puter controlled MTS machine equipped with a Research Incorporated radiant furnace controlled by a Leeds and Northrup temperature programming system. All the torsion tests were performed in a high purity argon atmosphere to minimize oxidation. Further details of this apparatus are presented elsewhere [8]. Stress-strain curves were determined from the torque-twist behavior in the usual manner [9].

The specimens were reheated at 1260°C for 15 min prior to execution of the torsion tests and all the passes were run at an equivalent strain rate of 2s<sup>-1</sup>. Two types of rolling schedule were employed in the laboratory simulations. The first was of the plate rolling type (designated as P) and consisted of 17 passes, each of 0.3 strain with a 30 s delay time between successive passes. During these tests, the temperature was continually decreased at a rate of 1°C/s, and the passes were executed between 1260 and 750°C. The purpose of these tests was to determine the three critical temperatures of the steels with respect to hot deformation, that is the  $T_{nr}$  or no-recrystallization temperature, the  $A_{r3}$  or start of the austenite-to-ferrite transformation on cooling, and the  $A_{r1}$  or end of the austenite-to-ferrite transformation on cooling. Concurrently, the dependence of flow stress on temperature under long interpass time conditions was also determined.

The second type of simulation involved three modified strip rolling schedules. These differed from one another only with respect to the finishing passes. The common roughing passes employed are described in Table 2 and the three finishing schedules are presented in Table 3. The first strip schedule (designated as S1) involved five finishing

**TABLE 2. Strip Rolling Roughing Schedule**

Pass No.	Strain	Interpass time (s)
R1	0.23	3.5
R2	0.25	8
R3	0.23	10
R4	0.29	12
R5	0.39	13
R6	0.67	18
R7	0.55	150

passes, and is based on strip rolling practice at the Lake Erie Works of Stelco Steel (Table 4 shows the average schedule used at the Lake Erie Works [5]). The second schedule (designated as S2) has the same number of passes and the same interpass times as schedule S1, but the strain in each of the last three finishing passes was increased to 0.55. One more finishing pass with a strain of 0.55 and an interpass time of 0.8 s was added to schedule S2 and led to the third strip schedule (designated as S3). As can be seen from Table 3, the total finishing strain increased from 2.1 in S1 to 3.2 in S3. These three schedules were employed to clarify the effect of increasing the total finishing strain on the microstructural evolution of such IF steels during hot rolling.

For the simulated strip rolling schedules, two different cooling cycles after deformation were used (Figure 1). As can be seen from this figure, one set of specimens was quenched into iced brine immediately after the last pass and the second set was air cooled at 8-10°C/s. The delay time between the last finishing pass and quenching was less than 2s.

The specimens were then mounted and polished so that the subsurface of the gauge length was just revealed. The quenched specimens were etched in hot saturated aqueous picric acid with a small addition of HCl and a wetting agent in order to reveal the prior austenite grain boundaries. For the air cooled specimens, a combination of 2% nital and picral was employed to reveal the final ferrite microstructure. The grain sizes were determined using standard linear intercept measurement techniques.

**TABLE 3. Strip Rolling Finishing Schedules**

Pass No.	S1	S2	S3	Interpass time(s)
	Strain	Strain	Strain	
F1	0.41	0.41	0.41	3.5
F2	0.57	0.57	0.57	2.5
F3	0.42	0.55	0.55	1.7
F4	0.4	0.55	0.55	0.8
F5	0.3	0.55	0.55	0.8
F6	-	-	0.55	0.8
Total Strain	2.1	2.6	3.2	-

## RESULTS AND DISCUSSION

### Behavior of the Two IF Steels Under Plate Rolling Conditions

Typical stress strain curves determined on IF steels A and B are displayed in Figures 2(a) and 2(b). In the austenite temperature range, steel A exhibited almost full static recrystallization during the interpass time, so that the pass-to-pass increase in flow stress was caused mainly by the decrease in temperature. Because of the small difference between the  $A_{r3}$  and  $A_{r1}$  temperatures in the IF steels, the austenite-to-ferrite transition is accompanied by a very sharp drop in flow stress (almost 50%). The increase in flow stress in the last few passes indicates that the transformation is complete and that strain accumulation is taking place in the ferrite.

According to the method of Boratto et al. [10] the critical temperatures in these steels can be determined by plotting the mean flow stress associated with each pass against the inverse absolute temperature, as shown in Figures 3(a) and 3(b) for steels A and B, respectively. As can be seen in Figure 3(a), steel A does not exhibit a  $T_{nr}$

**TABLE 4. Average Schedule Used for the Strip Rolling of IF Steels at the Lake Erie Works of Stelco Steel [5].**

Pass#	Equivalent strain per pass	Temperature (°C)	Delay time between passes (s)	Strain rate ( $s^{-1}$ )
R1	0.18	1280	3.7	3
R2	0.24	1268	11	4
R3	0.23	1255	10	6
R4	0.29	1238	12	7
R5	0.39	1213	13	10
R6	0.76	1185	18	15
R7	0.56	1130	40-200	21
F1	0.41	991-983	3.44-2.55	15
F2	0.53	980-953	2.25-1.6	30
F3	0.4	977-945	1.52-1.14	66
F4	0.37	972-930	1-0.8	85
F5	0.27	957-910	Coiling	115

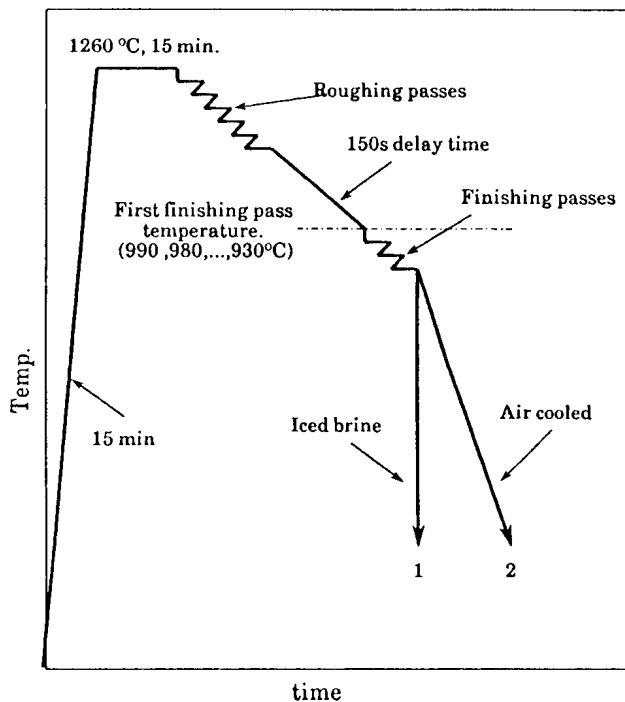


Figure 1. Cooling cycles followed in the present work.

under plate rolling conditions, but displays clear values for  $A_{r3}$  and  $A_{r1}$ . For steel B, (Figure 3(b)), the flow behavior up to the last two passes in the austenite region is similar to that displayed by the Ti-stabilized steel; however, there is a rapid increase in flow stress in the last two passes. This can be related in part to the solute drag of niobium and more especially to the precipitation of Nb carbonitride that occurs during the last 30 s interpass time above the  $A_{r3}$ .

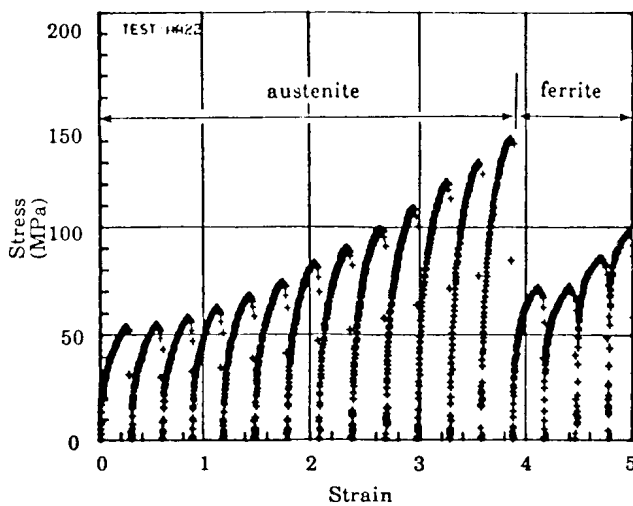


Figure 2(a). Stress-strain curves for steel A rolled according to the plate schedule.

These prevent both static and dynamic recrystallization and result in the rapid accumulation of work hardening.

The  $T_{nr}$  for steel B obtained from this method is 960°C and the values of  $A_{r3}$  and  $A_{r1}$  for this steel are approximately the same as for steel A, i.e. 890 and 860°C, respectively.

### Behavior of the Two IF Steels Under Strip Rolling Conditions

#### Roughing

As mentioned earlier, the roughing schedule was common for all three strip rolling schedules used in the present work. Typical stress-strain curves representing the seven roughing passes are illustrated in Figure 4(a). At passes 6 and 7, the two steels exhibited marked flow softening after reaching the maximum stress. This softening indicates that dynamic recrystallization was initiated during these passes [11,12]. The flow curves also show that a high degree of static softening takes place between passes; this can be attributed mainly to the occurrence of static recrystallization during the interpass times.

The mean flow stress versus inverse absolute temperature curves for the roughing passes are displayed in Figure 4(b). As can be seen from the figure, the mean flow stresses of the niobium stabilized steel are consistently higher than those of the titanium stabilized grade, the difference being ~10 MPa. This is because the solid solution strengthening effect of Nb is much stronger than that of Ti [13].

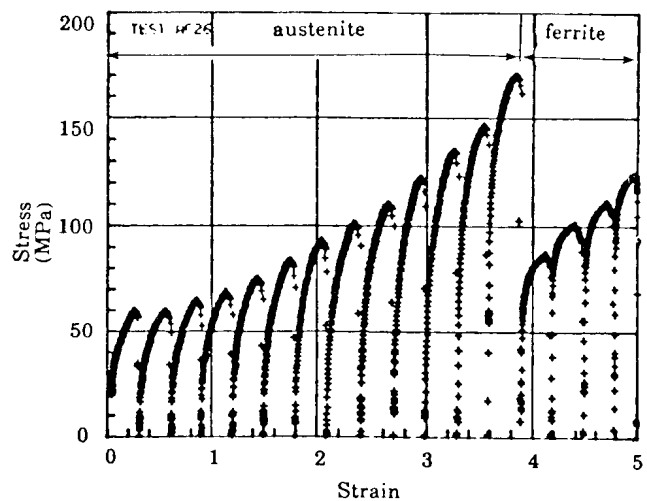


Figure 2(b). Stress-strain curves for steel B rolled according to the plate schedule.

### Finishing

An example of the flow curves for steel B finish rolled according to schedule S3, with a first finishing pass temperature of 930°C, is shown in Figure 5(a). (It should be recalled that this steel exhibited a  $T_{nr}$  of 960°C under plate rolling conditions.) As can be seen, there is an accumula-

tion of work hardening from the first finishing pass to the second, but after that, the maximum flow stress remains about the same. The lack of increase in flow stress with decreasing temperature indicates that dynamic recrystallization is taking place during deformation, followed by metadynamic recrystallization [12].

To confirm that dynamic recrystallization occurred during the finishing passes, a test was performed in which all the finishing passes were executed isothermally at 930°C (Figure 5(b)). The maximum stress is here followed by flow

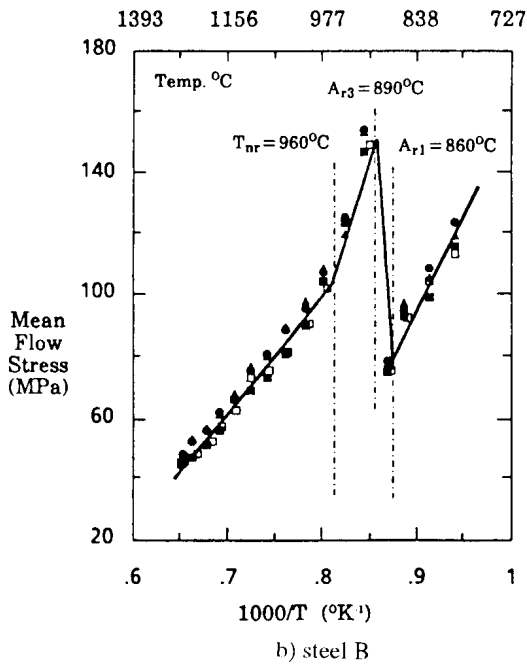
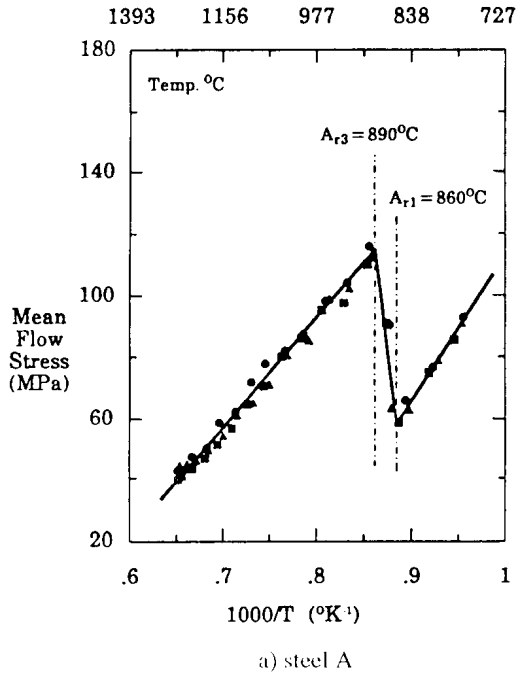


**Figure 3.** Dependence of mean flow stress on inverse absolute temperature for IF steels A and B rolled according to the plate schedule.

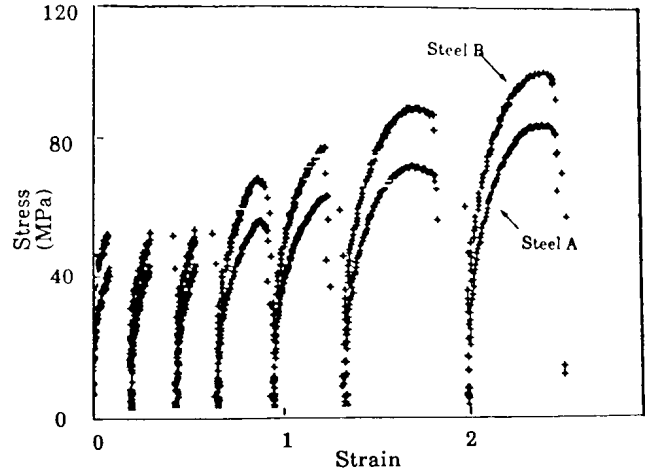


**Figure 4(a).** Flow curves for IF steels A and B rolled according to the strip roughing schedule.

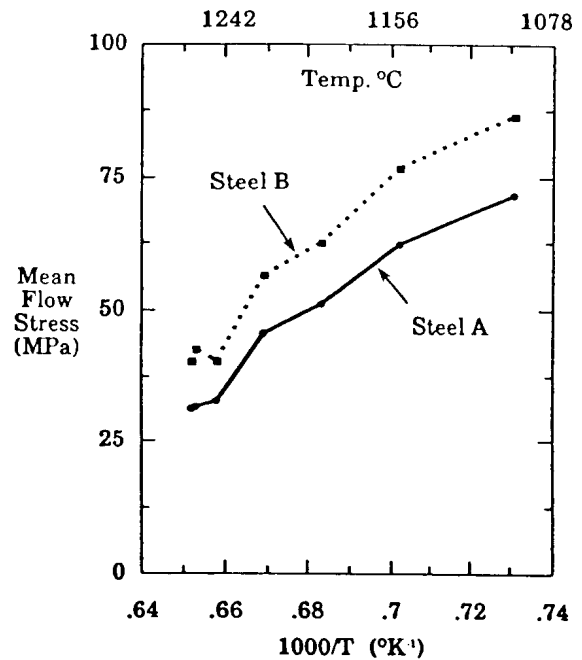


**Figure 4(b).** Dependence of mean flow stress on inverse absolute temperature of IF steels A and B during the seven prouging passes of the strip rolling schedules.

softening, as revealed by the envelope of the curves, which is a characteristic of dynamic recrystallization.

Finishing flow curves for steel A, deformed under the same conditions as for steel B, are displayed in Figures 6(a) and (b). (This steel did not exhibit a  $T_{nr}$  under plate rolling conditions.) From these figures, it appears that steel A also underwent dynamic recrystallization in the finishing passes, and that it exhibits a  $T_{nr}$  under the strip rolling (i.e. short

interpass time) conditions. Thus steel A exhibits a  $T_{nr}$  when strip rolling, but not plate rolling interpass times are used; and the strain is accumulated and dynamic recrystallization initiated when the interstand intervals are short.

### Influence of the First Finishing Pass Temperature on the Mean Flow Stress

Figures 7(a) and 7(b) illustrate the influence of first finish-

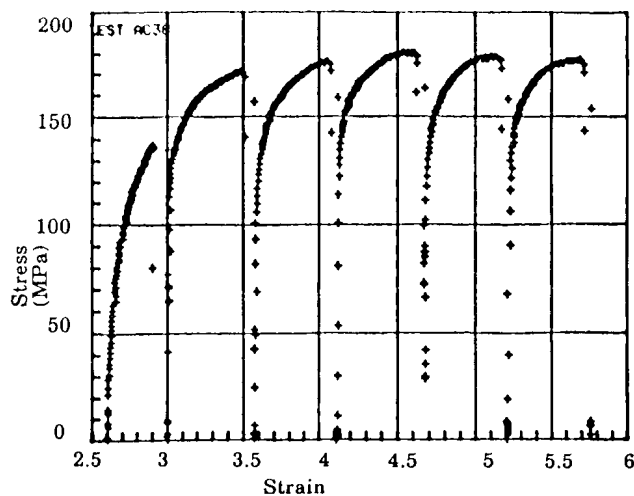


**Figure 5(a).** Finishing flow curves for steel B rolled according to strip rolling schedule S3 and with a constant finishing pass temperature of 930°C and 888°C.

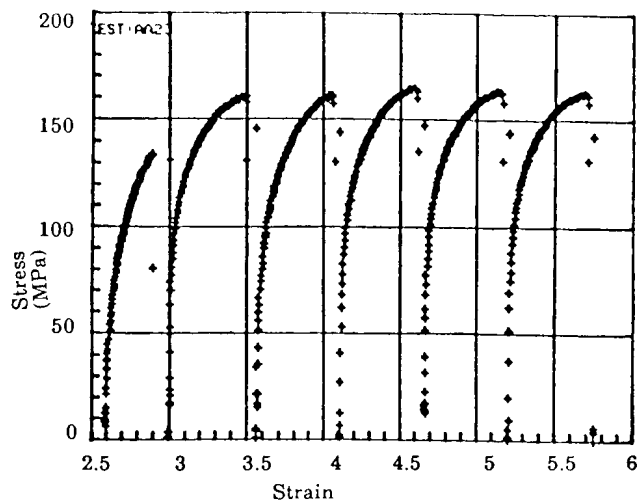


**Figure 6(a).** Finishing flow curves for steel A rolled according to strip rolling schedule S3 and with first and last finishing pass temperatures of 930°C and 888°C.

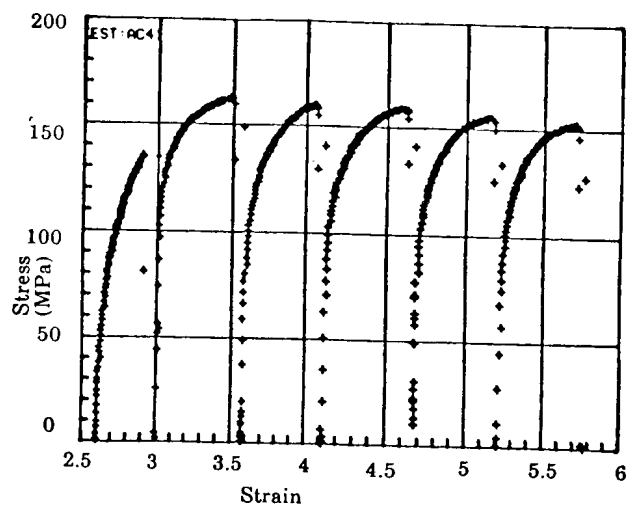


**Figure 5(b).** Finishing flow curves for steel B rolled according to strip rolling schedule S3 and with a constant finishing pass temperature of 930°C.

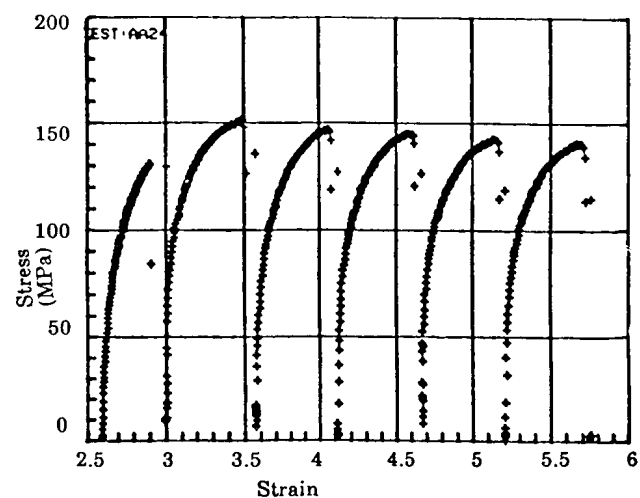


**Figure 6(b).** Finishing flow curves for steel A rolled according to strip rolling schedule S3 and with a constant finishing pass temperature of 930°C.

ing pass temperature on the mean flow stress for these IF steels. Figure 7(a) also shows the idealized behavior corresponding to the three types of recrystallization behavior: Type I takes place at relatively high temperatures and involves full static recrystallization between passes; this type corresponds to the recrystallization controlled rolling process (RCR). Type II refers to the absence of recrystallization and the rapid accumulation of work hardening; it occurs at temperatures below the  $T_{nr}$  and requires a chemistry and interpass times long enough to permit an appreciable amount of precipitation to take place. It corresponds to conventional controlled rolling (CCR) or the pancaking process. Type III takes place over the same temperature range as type II; however, in this case austenite pancaking is replaced by dynamic recrystallization during rolling. This type requires short delay times to reduce the amount of strain induced precipitation. Dynamic recrystallization leads to somewhat lower rolling loads than pancaking (type II), but to considerably higher loads than static recrystallization. This is because dynamic recrystallization does not remove dislocations as effectively as static

recrystallization, but still reduces the density below the levels present in fully work hardened (i.e. pancaked) austenite.

Once dynamic recrystallization is initiated, there is a break in the flow stress-temperature relationship and the stress level falls below that associated with pancaking. Such a break can be seen in Figure 7(a) for all the first finishing pass temperatures that were studied in this work. Thus, dynamic recrystallization was the main softening mechanism associated with the last four finishing passes. Comparison of the two diagrams indicates that the mean flow stresses associated with steel B are 10-25 MPa higher than for steel A.

It is also apparent that the behaviors of steel A, which does not have a  $T_{nr}$  under plate rolling conditions, and of steel B, which has a  $T_{nr}$ , are similar under strip rolling conditions. That is, there is a sharp increase in flow stress from F1 to F2, followed by a break in the flow stress-temperature relationship. As noted above, this behavior leads to the conclusion that both steels exhibit a  $T_{nr}$  when the interpass times are short, which is a approximately

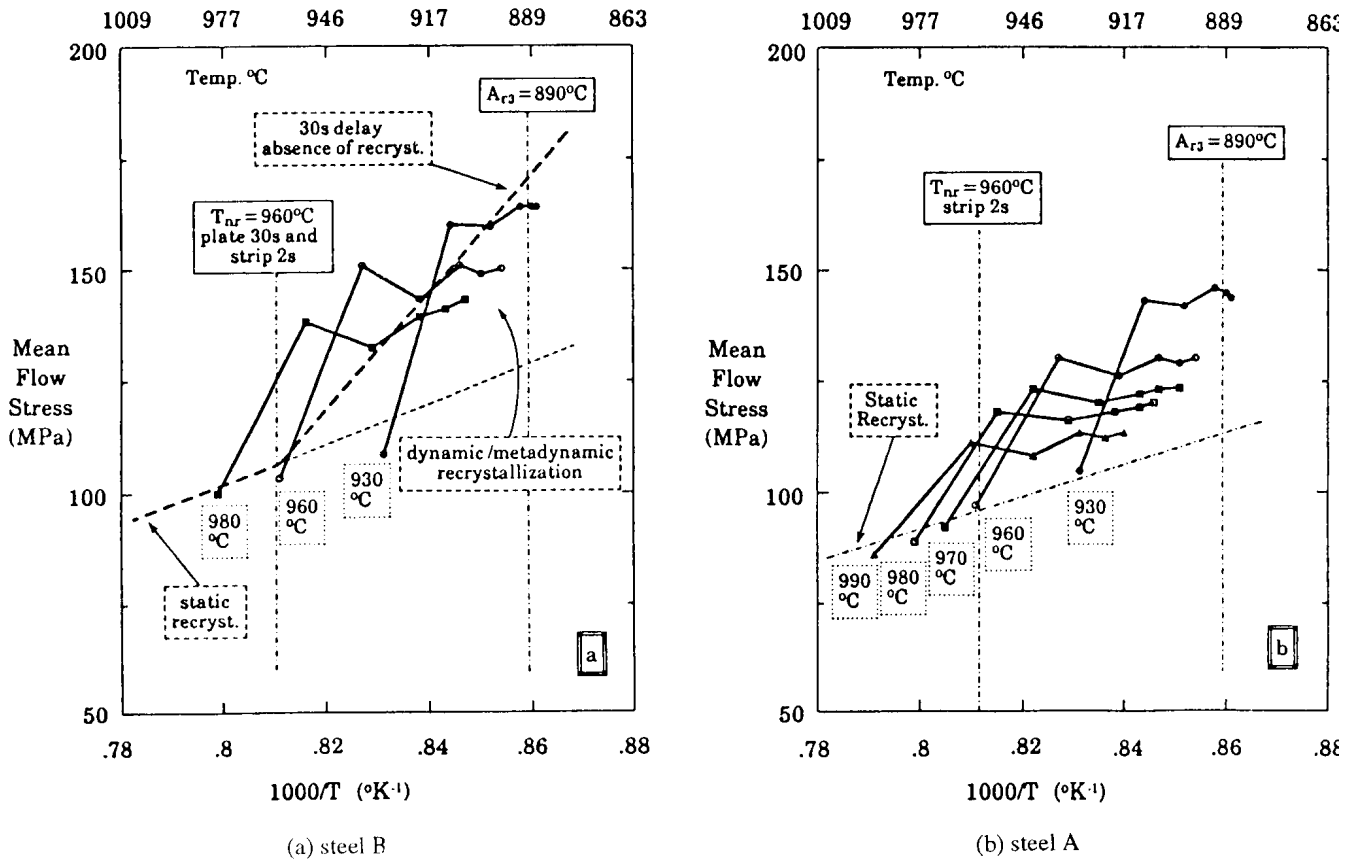


Figure 7. Influence of first finishing pass temperature on mean flow stress for steels B and A rolled according to the strip schedule S3.

960°C for both steels.

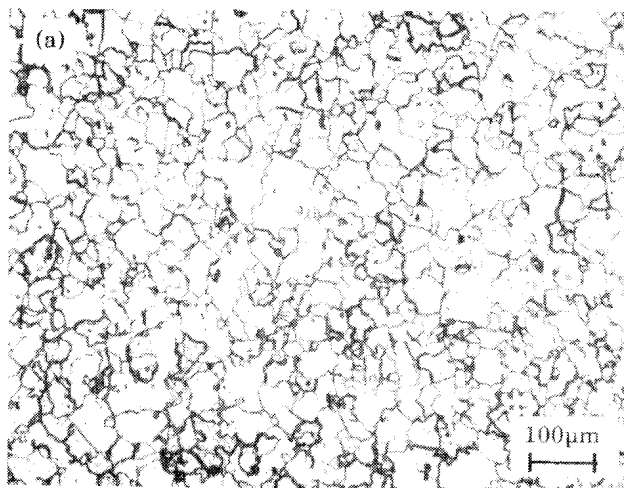
For the prediction of industrial rolling loads, the mean flow stress calculated for each pass must be corrected for the actual strain rates experienced in finishing mills using an equation of the form:

$$\bar{\sigma} = K\dot{\epsilon}^m \quad (1)$$

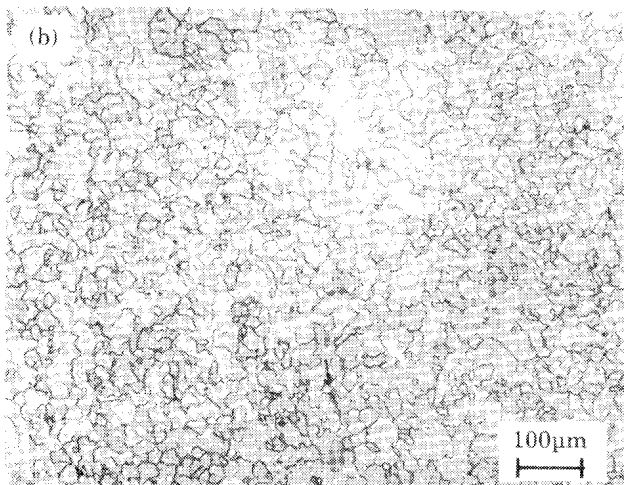
Here the strength coefficient  $K$  depends on strain, temperature, and material, and  $m$  is the strain rate sensitivity ( $\sim 0.08$  for IF steels in the finishing passes).

If  $\sigma_1$  and  $\sigma_2$  are the mean flow stresses at strain rates  $\dot{\epsilon}_1$  and  $\dot{\epsilon}_2$ , where  $\dot{\epsilon}_1$  is the simulation and  $\dot{\epsilon}_2$  the hot strip mill strain rate, equation (1) leads to the relation:

$$\frac{\sigma_2}{\sigma_1} = \left(\frac{\dot{\epsilon}_2}{\dot{\epsilon}_1}\right)^m \quad (2)$$



(a)  $\epsilon = 2.1$



(b)  $\epsilon = 2.6$

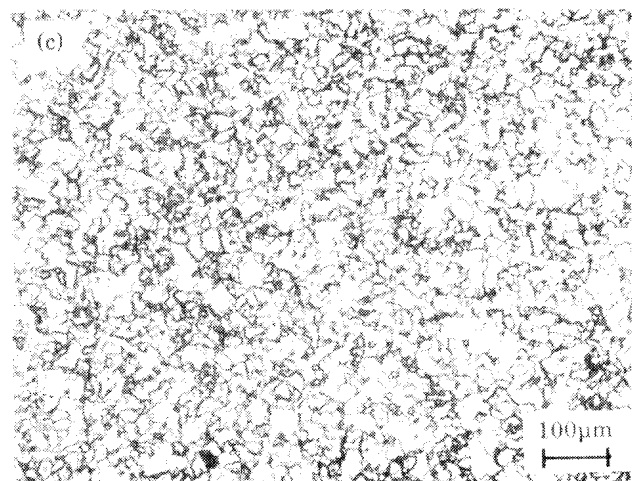
from which the expected rolling mill mean flow stress,  $\sigma_2$ , can be derived. (This relation was employed in the preparation of Figure 12 below).

### MICROSTRUCTURAL OBSERVATIONS

The influence of the total finishing strain on the *austenite* microstructure is shown in Figure 8. As can be seen from this figure, increasing the total finishing strain makes the grain size more uniform by enabling dynamic recrystallization to pass more completely through the microstructure. In this way, it also decreases the average austenite grain size [14]. It is of interest that dynamic recrystallization (followed by metadynamic recrystallization) takes place in steel A, which does not exhibit a conventional  $T_{nr}$ .

The effect of the finishing strain on the *ferrite* microstructure in steel A is displayed in Figure 9. Again it is clear that increasing the total finishing strain leads to a finer ferrite grain size [4,15]. The effect of first finishing pass temperature on the final ferrite grain size of steel A is illustrated in Figure 10. As expected [7], lowering the first finishing pass temperature decreases the ferrite grain size.

The ferrite grain sizes of the two IF steels are plotted against the inverse first finishing pass temperature in Figure 11. From this diagram, it is evident that, for a given finishing temperature, steel B has a finer ferrite grain size than steel A. This can be related to the stronger solute drag effect of Nb than of Ti [16]. Furthermore, TiN and TiC start to precipitate at higher temperatures than NbC and NbN. Thus, the Nb precipitates should be finer and more effective with respect to retarding grain boundary movement



(c)  $\epsilon = 3.2$

**Figure 8.** Effect of amount of total finishing strain on the austenite grain size of steel A (first finishing pass temp. =990°C



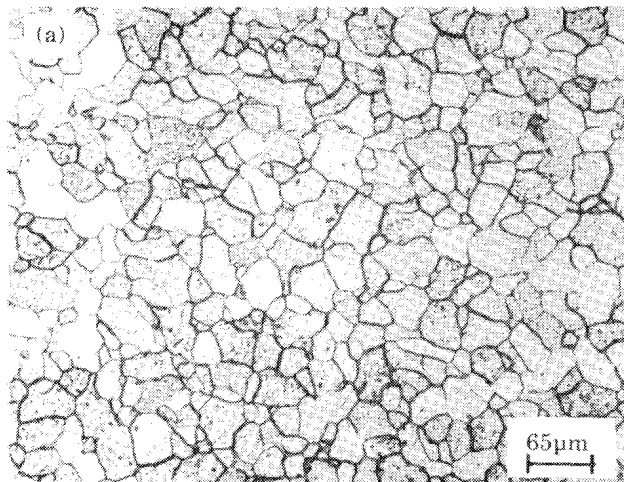
[17,18] than the Ti ones.

The relationship between the average mean flow stress of the last four finishing passes and the ferrite grain size for the two IF steels is illustrated in Figure 12. This figure shows that an increase in the mean flow stress leads to a decrease in the ferrite grain size, a trend which can be attributed to the effect of the higher density of dislocations on refining the austenite microstructure. The relationship between these two factors may be written as follows:

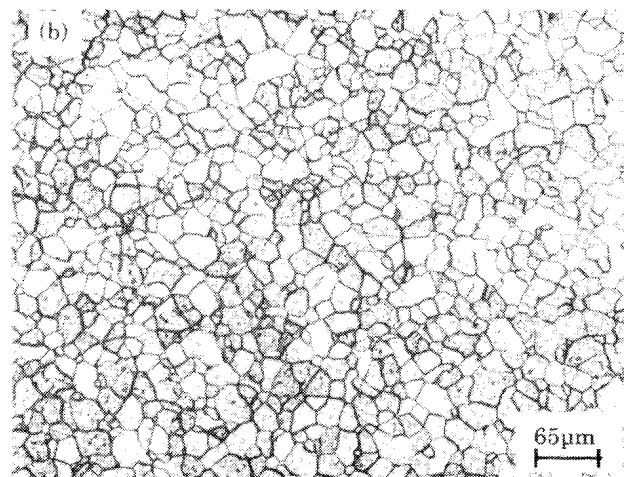
$$d = k(\sigma)^{-\alpha} \quad (3)$$

where  $d$  is the average ferrite grain size ( $\mu\text{m}$ ),  $\sigma$  is the mean flow stress (MPa), and  $k = 1.6 \times 10^5$  and  $\alpha = 1.83$  are constants.

With the aid of Equation (2) and setting  $m = 0.08$ , the

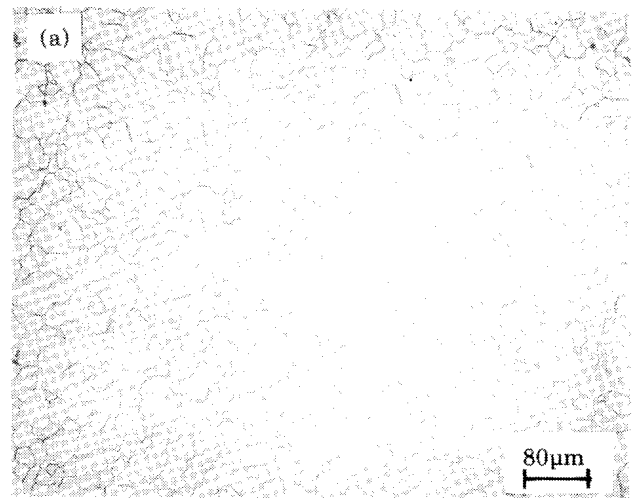


(a)  $\epsilon = 2.1$

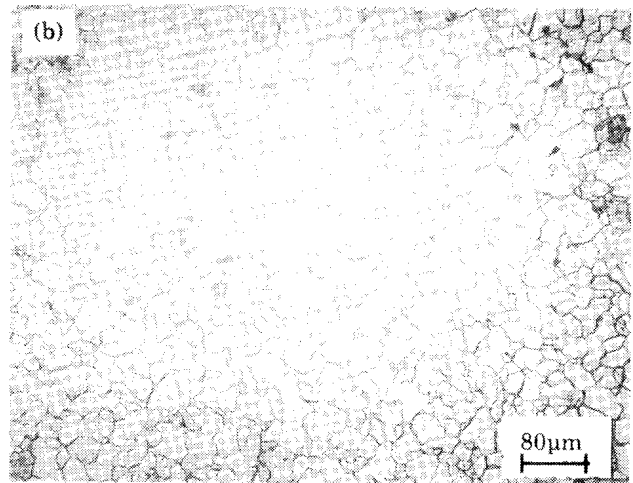


(b)  $\epsilon = 3.2$

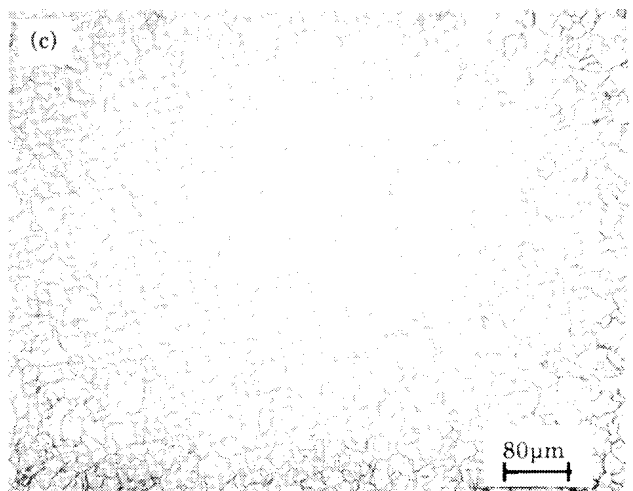
**Figure 9.** Effect of total finishing strain on the ferrite grain size of steel A (first finishing pass temp. = 960°C). Cooling rate of ~5°C/s



(a) FT = 990°C



(b) FT = 970°C



(c) FT = 930°C

**Figure 10.** Dependence of ferrite grain size of steel A ( $\epsilon = 3.2$ ) on first finishing pass temperature (FT).

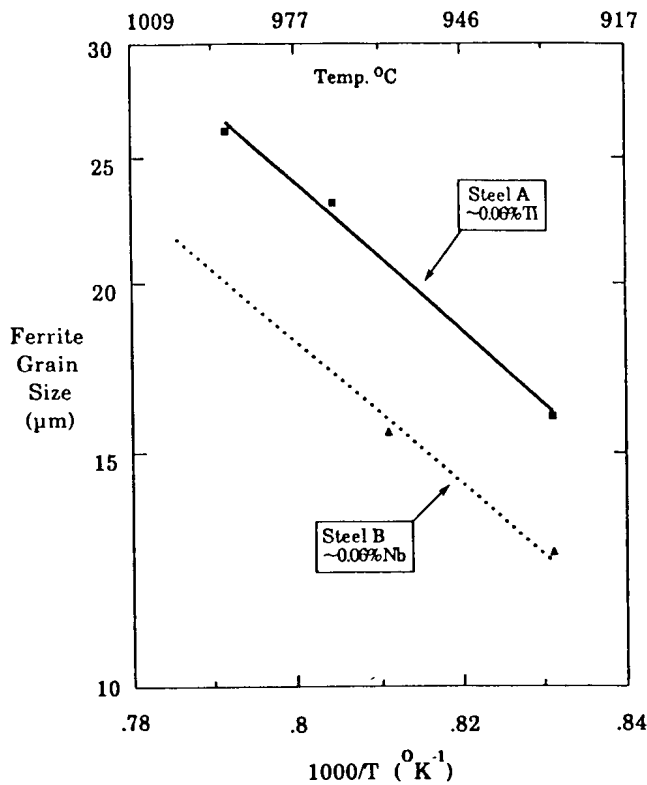


**Figure 11.** Influence of first finishing pass temperature on ferrite grain size. (S3 schedule)

expected mean flow stresses applicable to strip mill conditions were calculated. These values were used to estimate the average grain sizes that should be achieved under strip rolling conditions. These results are also displayed in Figure 12, where the simulations are represented by full squares and triangles for steels A and B, respectively, and the expected strip mill values by open squares and triangles, respectively. Simulations 1, 2 and 3, carried out on steel A, corresponded to mill entry temperatures of 990, 970 and 930°C, and simulations 4 and 5 on steel B to mill entry temperatures of 960 and 930°C. As can be seen from the figure, a first finishing pass temperature of 945°C is expected to lead to ferrite grain sizes of 11.5 and 9 µm, respectively, for steels A and B.

### CONCLUSIONS

The principal conclusions related to the present work are the following.

#### Plate rolling schedule

1. Under plate rolling conditions steel A, with 0.065%Ti,

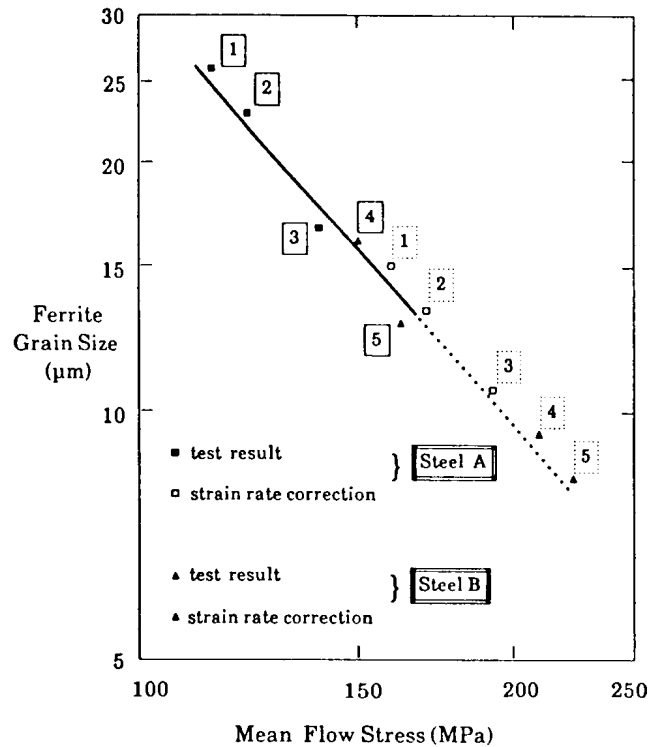


**Figure 12.** Relationship between the average flow stress of the last four finishing passes and the ferrite grain size. (S3 schedule).

does not exhibit a no-recrystallization ( $T_{nr}$ ) temperature, whereas steel B, with 0.056% Nb, exhibits clear ( $T_{nr}$ ) of 960°C.

2. The start and finish temperatures of the austenite-to-ferrite transformation are the same in the two steels, with  $A_{r3} = 890^\circ\text{C}$  and  $A_{r1} = 860^\circ\text{C}$ .

#### Strip rolling schedules

1. Under strip rolling conditions, complete static recrystallization takes place after each roughing pass. During the later finishing passes, there is retained work hardening, and dynamic recrystallization occurs to a degree that depends on the composition of the steel and the finishing temperature.
2. The mean flow stresses of the niobium stabilized steel are 10-25 MPa higher than those of the titanium-stabilized grade.
3. For both steels, increasing the total finishing strain and/or lowering the finishing pass temperatures decreases the ferrite grain size. Subjected to the same strip rolling schedule, the niobium stabilized steel has a finer ferrite grain size than the titanium stabilized grade and it is

expected that grain sizes as fine as 9  $\mu\text{m}$  can be attained at strip mill strain rates when the lowest possible finishing temperatures are used.

### ACKNOWLEDGEMENTS

A. Najafi-Zadeh expresses his thanks to the IUT for granting a period of sabbatical leave during which this work was carried out. The authors are indebted to K.R. Barnes of Stelco Steel for supplying the material and information about the rolling schedules. They acknowledge with gratitude the financial support received from the Natural Sciences and Engineering Research Council of Canada, the Quebec Ministry of Education (FCAR) program, and the Canadian Steel Industry Research Association (CSIRA).

### REFERENCES

1. I. Gupta, T. Porayil and L. T. Shiang "Hot and Cold Rolled Steel Sheets" TMS-AIME, Cincinnati, Ohio, 139-152 (1987).
2. S. Satoh, T. Obara, M. Nishida, and T. Irie Technology of Continuously Annealed Cold Rolled Sheet Steel, TMS-AIME, Warrendale, PA, 151 (1985).
3. I. Gupta and D. Bhattacharya TMS Fall meeting, Metallurgy of Vacuum-Degassed Steel Products, Indianapolis, Indiana, 43 (1989).
4. A. Najafi-Zadeh, J.W. Bowden, F.H. Samuel and J. J. Jonas. CIM, 29th Annual Conf. of Metallurgists, Hamilton, Ontario, August 26-30, paper no. 40.8. (1990).
5. F.H. Samuel, S. Yue and J.J. Jonas: TMS Fall Meeting, Metallurgy of Vacuum-Degassed Steel Products, Indianapolis, Indiana, 395 (1989).
6. O. Hashimoto, S. Satoh, T. Irie and N. Ohashi. Proc. of the Int. Conf. on Advances in Physical Metallurgy and Applications of Steel, The Metals Society, 95 (1984).
7. W. Bleck, R. Bolde and F.J. Haben, TMS Fall Meeting, Metallurgy of Vacuum-Degassed Steel Products, Indianapolis, Indiana, 73 (1989).
8. T. Chandra, S. Yue, J.J. Jonas and R.J. Ackert: Proc. 4th Int. Conf., The Science and Technology of Flat Rolling, Deauville, France, June, Vol 2, F18.1 (1987).
9. S.L. Semiatin, G. Lahoti and J.J. Jonas, ASM Metals Handbook, 9th Ed. ASM, pp. 154-184 (1985).
10. F. Boratto, R. Barbosa, S. Yue and J.J. Jonas: Proc. Int. conf. on Phys. Metall. of Thermomechanical Processing of Steels and Other Metals, (Thermec 88), 383 (1988).
11. T. Sakai, Y. Nagao, M. Ohashi and J.J. Jonas: *Materials Science and Technology*, 2, 659 (1987).
12. F.H. Samuel, S. Yue, J.J. Jonas and K.R. Barnes *ISIJ*, 30, 216, (1990).
13. M.G. Akben and J.J. Jonas Proc. Int. Conf. on HSLA, 3-6 Oct. Philadelphia, PA, 149 (1983).
14. J.J. Jonas and T. Sakai: Deformation Processing, and Structure, ASM Materials Science Seminar, ASM, 185 (1984).
15. R.I.L. Guthrie and J. J. Jonas: ASM Metals Handbook, 10th. Ed., ASM, pp. 107-125 (1989).
16. K. Tsunoyama, S. Satoh, Y. Yamazaki and H. Abe, TMS Fall Meeting, Metallurgy of Vacuum-Degassed Steel Products, Indianapolis, Indiana, 127 (1989).
17. R. P. Smith: *Trans. Met. Soc. AIME*, 236, 220 (1966).
18. A. Okamoto and N. Mizui, TMS Fall meeting, Metallurgy of Vacuum-Degassed Steel Products, Indianapolis, Indiana, 61 (1989).